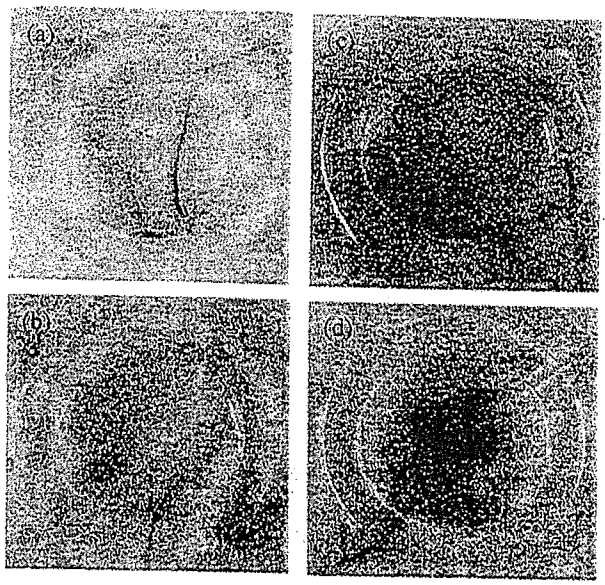

Figure 12.2 Skin angiogenesis in the DAS model usage of a DAS model in PDT is shown. Saline-loaded (a) or Meth-A sarcoma (1×10^7 cells/0.15 ml)-loaded (b–d) chamber rings were dorsally implanted into BALB/c mice. At 4 days after implantation of the chamber ring, PDT treatment was performed by an i.v. injection of saline (a, b) or Visudyne®, 0.25 mg/kg in terms of BPD-MA (c, d). The animals were exposed to a laser light of 689 nm with 150 J/cm^2 of fluence at 15 min (c) or 3 h (d) post-injection of Visudyne®. At 24 h after PDT treatment, the mice were sacrificed; and the neovascularized dorsal skin was resected for observation. Data reproduced with kind permission from *Cancer Letters*, Ichikawa *et al.*, 2004.

photodamage of the angiogenic site was dramatically increased (Figure 12.2c). In contrast, no significant change was observed after 3-h PDT (Figure 12.2d). These results suggest that the enhanced anti-tumour activity after 15-min PDT is mainly introduced by endothelial cell degeneration, leading to vascular haemorrhage rather than by tumour cell damage, although Visudyne® taken up by tumour cells as early as 15 min post-injection simultaneously may cause the cell death after laser irradiation.

12.4 Determination of blood volume or blood flow in the angiogenic site using the DAS model

The DAS method has recently been modified to measure blood volume in the angiogenesis-induced skin as determined by the amount of ^{51}Cr-labelled erythrocytes circulating in the skin (Funahashi *et al.*, 1999). Radiolabelling of erythrocytes is carried out by a simple incubation of erythrocytes with [^{51}Cr] sodium chromate. Kurohane *et al.* (2001) utilized this method to observe the effects of 15-min PDT on blood volume. In brief, erythrocytes freshly prepared from BALB/c

mice were incubated for 30 min at 37°C with 9.25 MBq of [^{51}Cr] sodium chromate (Daiichi Pure Chemical Co., Ltd., Tokyo, Japan). After washing, the radiolabelled erythrocytes were suspended in saline. The chamber-ring-bearing mice were prepared as described previously and allowed to develop for 4 days prior to PDT treatment. Fifteen minutes or 3 h after intravenous injection of liposomal BPD-MA (a sensitizer similar to Visudyne^{R}, with a different liposomal composition) into the DAS model mice, skins on the chamber rings were irradiated by a laser light. At 1, 6 and 24 h after PDT treatment, the mice were injected via the tail vein with ^{51}Cr-labelled erythrocytes (1×10^8 cells/0.2 ml). Control mice, namely those without treatment, those injected with saline and then irradiated, and those injected with liposomal BPD-MA without laser irradiation were also injected with ^{51}Cr-labelled erythrocytes. At 30 min after erythrocyte injection, the mice were sacrificed with diethylether anaesthesia, and the skin attached the chamber ring was cut away. The radioactivity of ^{51}Cr in the skin was measured using a gamma counter. ^{51}Cr accumulated in angiogenic skins 1 h after PDT (see Figure 12.3), indicating the erythrocytes were unable to flow away through the vessels, suggesting that there was endothelial cell damage. The flow of ^{51}Cr-labelled erythrocytes into the skin was recovered to the control level 24 h after 3-h PDT. On the other hand, complete suppression of blood flow was observed 24 h after 15-min PDT, suggesting that anti-angiogenic PDT causes haemostasis.

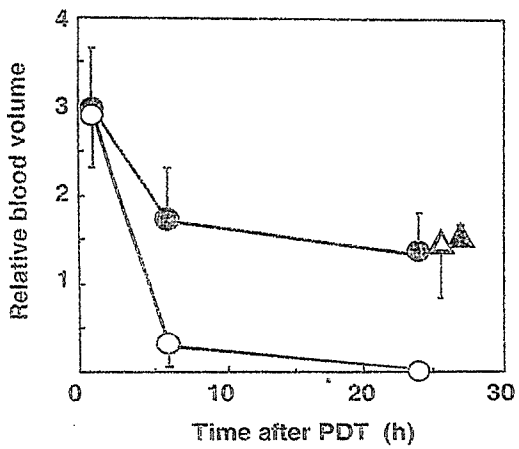

Figure 12.3 Blood volume change at the PDT-treated neovascular site meth a sarcoma cell-loaded chamber rings (1×10^7 cells/0.15 ml) were implanted into the dorsal air sac of mice. Day 4 after the implantation, the mice were injected *via* a tail vein with 2 mg/kg of liposomal BPD-MA. Then the mice were kept in the dark for 15 min (open circles) or 3 h (closed circles) before irradiation with 689 nm laser light (150 J/cm^2). At 1, 6, or 24 h after the irradiation, the mice were injected *via* a tail vein with ^{51}Cr-labelled erythrocyte (1×10^8 cells/0.2 ml). Thirty minutes post-injection, the PDT-treated neovascularized skin was removed and the radioactivity was then counted with a gamma counter. Blood volume is presented as ratio of treated to control values. Each point represents the mean ± S.D. ($n = 4$). Open triangle, laser irradiation alone; closed triangle, liposomal BPD-MA injection without laser irradiation. Data reproduced with kind permission from *Cancer Letters*, Kurohane *et al.*, 2001.

12.5 Quantitative or semi-quantitative analysis of angiogenesis in the DAS model

For qualitative analysis of angiogenesis, the skin attached to the chamber ring of a DAS model is examined with naked eyes or under a microscope. Imaging software enables quantification of vessel density using photographs of angiogenic skins, however, it is sometimes difficult to subtract pre-existing vessels from this analysis. In contrast, the Evans blue method is quite easy and useful for semi-quantitative evaluation of angiogenesis. This method utilizes the fact that the endothelial cell layer of angiogenic neovessels is characteristically weak and leaky. Since angiogenic vessels are leaky enough to allow outflow of the dye, Evans blue accumulates in the interstitial spaces around the neovessels, but does not leak out from pre-existing vessels. Therefore, the amount of accumulated dye between angiogenic skin and control skin is quite different.

The Evans blue is used by intravenous injection of 0.2 ml of 1 per cent (w/v) Evans Blue (Wako Pure Chemical, Osaka, Japan) in phosphate-buffered saline (PBS), pH 7.4, into the DAS bearing mice via the tail vein, 4–5 days after ring implantation. One minute after injection, the mice are sacrificed under anaesthesia and the angiogenic skin is detached. The skin is then frozen on dry ice and cut along the chamber ring. The pigment in the skin attached to the chamber ring is extracted using 0.15 per cent Na_2SO_4-70 per cent acetone for 1 h at room temperature. The extracted solution is then centrifuged at 12 000 x *g* for 1 min, and the absorbance of the supernatant is determined at 620 nm.

Yamakawa *et al.* (2004) applied this Evans blue method for evaluating the anti-angiogenic effect of a tea polyphenol, (–)-epigallocatechin gallate (EGCG), in the DAS model. Matrix metalloproteinases (MMPs) are known to play an important role in endothelial cell invasion during angiogenesis and we reported that membrane type-1 MMP (MT1-MMP) activity was potentially suppressed by EGCG in Oku *et al.* (2003). Therefore, we examined the effect of EGCG on invasion and tube formation of endothelial cells *in vitro*, and on angiogenesis and tumour growth *in vivo*. The results of these experiments indicated that EGCG actually suppressed angiogenesis and tumour growth, potentially via the suppression of MT1-MMP. Treatment with EGCG in the DAS model showed a significant suppression of angiogenesis (Figure 12.4). In this experiment a chamber ring loaded with HT1080 human fibrosarcoma cells was prepared and implanted dorsally into 5-week-old BALB/c male mice. EGCG (40 mg/kg, 0.2 ml/mouse/day) or PBS was injected intravenously into a tail vein for 4 days from the day of implantation. At day 4 after ring implantation, the skin attached to the chamber ring was surgically removed, and the degree of neovascularization was semi-quantified by Evans blue method. Negative controls were obtained utilizing mice implanted with medium-loaded chamber rings. A strong induction of angiogenesis was observed when HT1080 fibrosarcoma cells were loaded into the chamber rings (Figure 12.4a), in contrast to the controls where implantation of

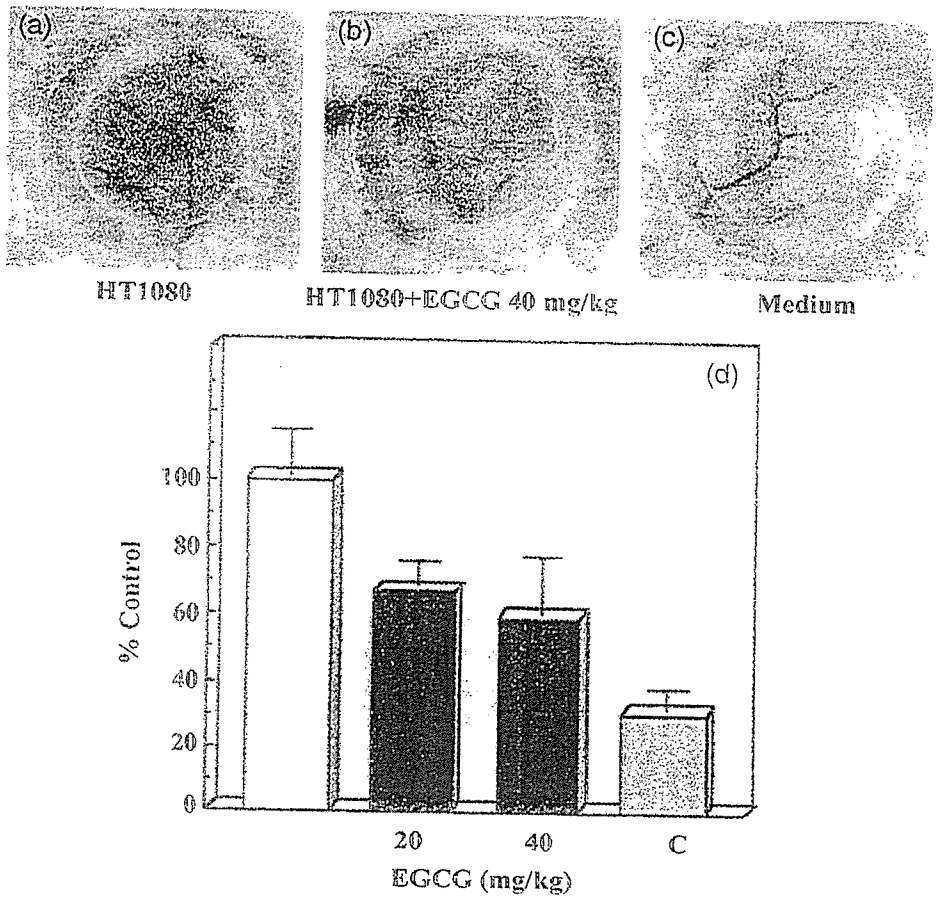

Figure 12.4 Suppression of angiogenesis with EGCG treatment a chamber ring loaded with HT1080 fibrosarcoma cells (a, b) or with medium alone (c) was dorsally implanted into mice. The mice were injected with 0.2 ml of EGCG (40 mg/kg, b) or PBS (a, c) everyday from day 0 to day 3 after implantation of the chamber ring. At day 4, mice were sacrificed and the attached skin on the chamber ring was observed. d, A chamber ring loaded with HT1080 fibrosarcoma or with medium alone was similarly implanted as negative control (shadow bars). The mice were injected with 0.2 ml of EGCG (closed bars) or PBS (open bars) everyday from day 0 to day 3 after implantation of the chamber ring. At day 4, Evans blue was injected into the mice and at 1 min after the injection, they were sacrificed and the attached skin on the chamber ring was cut out. The pigment was extracted with 0.15 per cent Na_2SO_4-70 per cent acetone and measured absorbance at 620 nm. Data are presented as mean +/− SEM. Data reproduced with kind permission from *Cancer Letters*, Yamakawa *et al.*, 2004.

a medium-loaded chamber ring did not induce angiogenesis (Figure 12.4c). EGCG treatment (40 mg/kg/day) resulted in suppression of angiogenesis (Figure 12.4b). Corresponding to these observations, accumulation of Evans blue in the angiogenic skin was reduced in EGCG-treated group (40.6 per cent reduction in this experiment) compared with PBS controls (Figure 12.4d).

12.6 Isolation and application of neovessel-targeting probe using DAS model

As tumours are dependent upon angiogenesis, disruption of this process proves an attractive target for the development of potential therapies. Current anti-cancer drugs cause damage to growing cells thereby affecting the neovessels as well as the tumour cells. We previously proposed that anti-neovascular therapy, whereby neovessel-targeted drug carriers are used to deliver anti-cancer drugs to angiogenic endothelial cells, may prove effective in cancer treatment via indirect lethal damage to tumour cells through damage to neovessels, which would block the supply of oxygen and nutrients to the tumour cells. For this purpose, we designed liposomes modified with a neovessel specific probe as drug carriers, and we isolated peptides specific for tumour angiogenic vasculature as the probe molecules by using a phage-displayed peptide library, described in Oku *et al.* (2002). *In vivo* biopanning of phage-displayed peptide library was performed in angiogenic model mice prepared by a DAS method (see Figure 12.5). In this experiment, a DAS model was quite advantageous because it enabled us to isolate specific phage clones having the ability to bind only to angiogenic vessels, not to tumour cells.

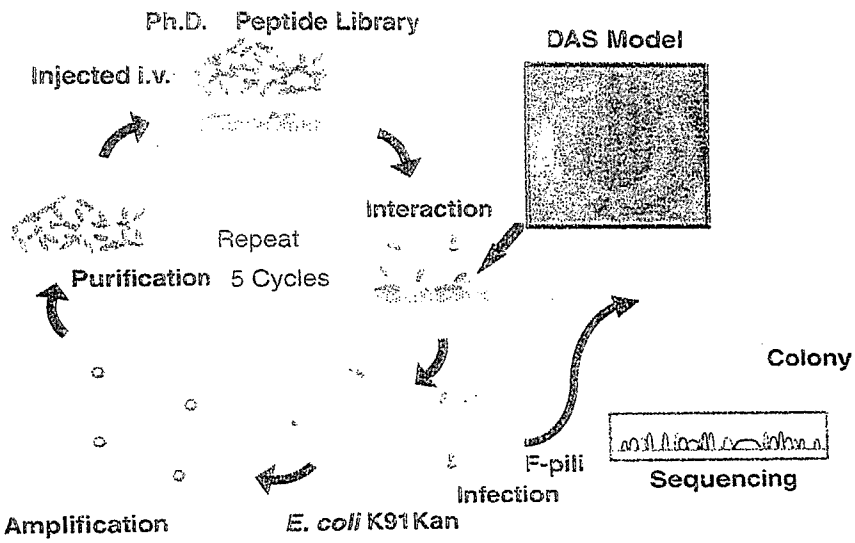

Figure 12.5 *In vivo* biopanning by using a DAS model the DAS model mice were prepared by using highly metastatic murine B16BL6 melanoma cells (1×10^7 cells/ring). Five days after implantation, these mice were used for *in vivo* biopanning. A phage-displayed random peptide library expressing pentadecapeptides at the N terminus of pIII coat protein of M13 phage was injected into the DAS model mice via a tail vein. Four minutes after injection, the phages that had accumulated in angiogenic vessels were recovered and titrated. Biopanning steps were repeated for five cycles. After selected phages were cloned, sequences of the presented peptides were determined. The purified peptides obtained by this method potentially associate with neovessels. (A colour reproduction of this figure can be viewed in the colour section towards the centre of the book).

After determination of the epitope sequences of the obtained phage clones, APRPG-modified liposome was revealed to be favourable for the active targeting of the angiogenic endothelium. Furthermore, Maeda *et al.* (2004) reported that anti-neovascular therapy using this type of liposome as a carrier of adriamycin markedly suppressed tumour growth possibly through a cytotoxic effect of the drug against angiogenic endothelial cells.

12.7 Conclusions

The advantages of a DAS model are that this approach is simply carried out without special skills, tumour-induced angiogenesis is reproduced in natural environment, and tumour cells derived from different species, including human, can be used in conventional mice since the cells loaded in a chamber ring would not be recognized by the host immune system. In contrast, variability in the amount of pre-existing vessels where the chamber ring is implanted affects the evaluation of angiogenesis such as blood flow determination. In some cases, it is difficult to evaluate the degree of angiogenesis by qualitative observations, although advances in the use of image analysis software to view vessels are making interpretation of results easier. It is possible actually to observe or count vessels by eye, but angiogenic vessels vary in diameter and length as well as number so quantification by eye minimizes the effects seen with individual treatments. Although the methods described above are indirect, they allow for greater interpretation of results. The activity of anti-angiogenic substances is easily examined by using DAS models and this methodology is useful for development of anti-angiogenic drugs or anti-angiogenic therapies. Moreover, DAS model can be modified for analysis of the mechanisms of angiogenesis. For example, implantation of a chamber ring loaded with tumour cells manipulated to over- or under-express certain factors will help reveal the role of the relevant test factor in angiogenesis.

A recent development in the DAS method has taken this one step further by pre-loading the ring with a single test peptide rather than tumour cells, which will secrete a number of different factors. Hamada *et al.* (2004) used this method to compare the effects of a test peptide with VEGF, a known pro-angiogenic protein. This novel use of the DAS assay might give new insight for understanding the mechanisms of angiogenesis stimulated by single test factors.

References

Asai, T., Shimizu, K., Kondo, M., Kuromi, K. *et al.* (2002) 'Anti-neovascular therapy by liposomal DPP-CNDAC targeted to angiogenic vessels', *FEBS Letters*, **250**(1–3), pp. 167–170.

Dolmans, D. E., Fukumura, D. and Jain, R. K. (2003) 'Photodynamic therapy for cancer', *Nature Rev. Cancer*, 3(5), pp. 380–387.

Funahashi, Y., Wakabayashi, T., Semba, T., Sonoda, J. *et al.* (1999) 'Establishment of a quantitative mouse dorsal air sac model and its application to evaluate a new angiogenesis inhibitor', *Oncol. Res.*, 11(7), pp. 319–329.

Hamada, Y., Yuki, K., Okazaki, M., Fujitani, W. *et al.* (2004) 'Osteopontin-derived peptide SVVYGLR induces angiogenesis in vivo', *Dental Materials J.*, 23(4), pp. 650–655.

Ichikawa, K., Takeuchi, Y., Yonezawa, S., Hikita, T. *et al.* (2004) 'Antiangiogenic photodynamic therapy (PDT) using Visudyne causes effective suppression of tumor growth', *Cancer Lett.*, 205(1), pp. 39–48.

Kurohane, K., Tominaga, A., Sato, K., North, J. R. *et al.* (2001) 'Photodynamic therapy targeted to tumor-induced angiogenic vessels', *Cancer Lett.*, 167(1), pp. 49–56.

Maeda, N., Takeuchi, Y., Takada, M., Sadzuka, Y. *et al.* (2004) 'Anti-neovascular therapy by use of tumor neovasculature-targeted long-circulating liposome', *J. Controlled Release*, 100(1), pp. 41–52.

Oikawa, T., Sasaki, M., Inose, M., Shimamura, M. *et al.* (1997) 'Effects of cytogenin, a novel microbial product, on embryonic and tumor cell-induced angiogenic responses in vivo', *Anticancer Res.*, 17(3C), pp. 1881–1886.

Oku, N., Asai, T., Watanabe, K., Kuromi, K. *et al.* (2002) 'Anti-neovascular therapy using novel peptides homing to angiogenic vessels', *Oncogene*, 21(17), pp. 2662–2669.

Oku, N., Matsukawa, M., Yamakawa, S., Asai, T. *et al.* (2003) 'Inhibitory effect of green tea polyphenols on membrane-type 1 matrix metalloproteinase, MT1-MMP', *Biol. Pharm. Bull.*, 26(9), 1235–1238.

Peng, Q., Warloe, T., Moan, J., Godal, A. *et al.* (2001) 'Antitumor effect of 5-aminolevulinic acid-mediated photodynamic therapy can be enhanced by the use of a low dose of photofrin in human tumor xenografts', *Cancer Res.*, 61(15), pp. 5824–5832.

Reuther, T., Kubler, A. C., Zillmann, U., Flechtenmacher, C. and Sinn, H. (2001) 'Comparison of the in vivo efficiency of photofrin II-, mTHPC-, mTHPC-PEG- and mTHPCnPEG-mediated PDT in a human xenografted head and neck carcinoma', *Lasers Surg. Med.*, 29(4), pp. 314–322.

Shimizu, K. and Oku, N. (2004) 'Cancer anti-angiogenic therapy', *Biol. Pharm. Bull.*, 27(5), pp. 599–605.

Takeuchi, Y., Kurohane, K., Ichikawa, K., Yonezawa, S. *et al.* (2002) 'Induction of intensive tumor suppression by antiangiogenic photodynamic therapy using polycation-modified liposomal photosensitizer', *Cancer*, 97(8), pp. 2027–2034.

Yamakawa, S., Asai, T., Uchida, T., Matsukawa, M. *et al.* (2004) '(−)-Epigallocatechin gallate inhibits membrane-type 1 matrix metalloproteinase, MT1-MMP, and tumor angiogenesis', *Cancer Lett.*, 210(1), pp. 47–55.

Biol. Pharm. Bull. **29**(9) 1936—1940 (2006) Vol. 29, No. 9

Enhancement of Anticancer Activity in Antineovascular Therapy Is Based on the Intratumoral Distribution of the Active Targeting Carrier for Anticancer Drugs

Noriyuki MAEDA,[a,b] Souichiro MIYAZAWA,[a] Kosuke SHIMIZU,[a] Tomohiro ASAI,[a] Sei YONEZAWA,[a] Sadaya KITAZAWA,[b] Yukihiro NAMBA,[b] Hideo TSUKADA,[c] and Naoto OKU*,[a]

[a] *Department of Medical Biochemistry and COE Program in the 21st Century, School of Pharmaceutical Sciences, University of Shizuoka; 52–1 Yada, Suruga-ku, Shizuoka 422–8526, Japan:* [b] *Nippon Fine Chemical Co., Ltd.; 5–1–1 Umei, Takasago, Hyogo 676–0074, Japan: and* [c] *Central Research Laboratory, Hamamatsu Photonics K.K.; 5000 Hirakuchi, Hamamatsu 434–8601, Japan.*

Received April 17, 2006; accepted June 22, 2006; published online June 28, 2006

We previously observed the enhanced anticancer efficacy of anticancer drugs encapsulated in Ala-Pro-Arg-Pro-Gly-polyethyleneglycol-modified liposome (APRPG-PEG-Lip) in tumor-bearing mice, since APRPG peptide was used as an active targeting tool to angiogenic endothelium. This modality, antineovascular therapy (ANET), aims to eradicate tumor cells indirectly through damaging angiogenic vessels. In the present study, we examined the *in vivo* trafficking of APRPG-PEG-Lip labeled with [2-^{18}F]2-fluoro-2-deoxy-D-glucose ([2-^{18}F]FDG) by use of positron emission tomography (PET), and observed that the trafficking of this liposome was quite similar to that of non-targeted long-circulating liposome (PEG-Lip). Then, histochemical analysis of intratumoral distribution of both liposomes was performed by use of fluorescence-labeled liposomes. In contrast to *in vivo* trafficking, intratumoral distribution of both types of liposomes was quite different: APRPG-PEG-Lip was colocalized with angiogenic endothelial cells that were immunohistochemically stained for CD31, although PEG-Lip was localized around the angiogenic vessels. These results strongly suggest that intratumoral distribution of drug carrier is much more important for therapeutic efficacy than the total accumulation of the anticancer drug in the tumor, and that active delivery of anticancer drugs to angiogenic vessels is useful for cancer treatment.

Key words cancer antineovascular therapy; long-circulating liposome; angiogenesis; active targeting; positron emission tomography (PET)

Angiogenesis is critical for maintenance, proliferation and hematogenous metastasis of tumor.[1,2] Recently, various antiangiogenic therapeutic modalities have accomplished remarkable progress. We previously proposed cancer antineovascular therapy (ANET)[3,4]: Indirect tumor regression is achieved through damaging neovessel endothelial cells by anticancer drugs, since neovessel endothelial cells are growing cells and are susceptible to anticancer drugs like as tumor cells. For this purpose, we isolated APRPG peptide specifically bound to tumor angiogenic vasculature from phage-displayed peptide library, and observed that APRPG-modified liposomes accumulated in tumor tissue higher than unmodified one in tumor-bearing mice. In addition, the liposomes encapsulating adriamycin (ADM) strongly suppressed tumor growth.[3] ANET is expected to suppress both primary tumor and metastasis without acquiring drug resistance. In fact, ADM-resistant P388 tumor was susceptible to ADM encapsulated in APRPG-modified liposomes.[5] The therapy is also expected for a broad spectrum of cancers.

On the other hand, it is known that polyethyleneglycol (PEG)-coated liposomes have long-circulating characteristics through avoidance of uptake by reticuloendothelial system (RES) such as liver and spleen,[6,7] because PEG-coating protects liposomes from opsonization and attack of lipoproteins by their surface aqueous layers.[8] Furthermore, PEG-coated liposomes are expected to accumulate in tumor tissue through leaky vasculature of angiogenic vessels by enhanced permeability and retention (EPR) effect.[9,10]

Therefore, we synthesized APRPG peptide attached to PEG termini of PEG-disteaoylphosphatidylethanolamine (PEG-DSPE) to prepare angiogenesis-targeted liposomes with long circulating characteristic.[11] We previously observed that ADM-encapsulated liposomes modified with APRPG-PEG caused more efficient tumor growth suppression than ADM-encapsulated liposomes modified with PEG alone in Colon 26 NL-17 carcinoma (C26 NL-17)-bearing mice, despite not so much different accumulation of both liposomes in the tumor.[12] To clarify the advantage of angiogenesis-targeted long-circulating liposomes, we examined the *in vivo* trafficking of APRPG-PEG-modified liposomes as well as non-modified or PEG-modified ones in tumor-baring mice with positron emission tomography (PET) in the present study: The method is able to determine the real time liposomal trafficking non-invasively.[13] Furthermore we investigated the intratumoral distribution of liposomes modified with APRPG-PEG by use of fluorescence-labeled liposomes, and observed that differential local distribution between APRPG-PEG-modified liposomes and those modified with PEG alone.

MATERIALS AND METHODS

Materials APRPG-PEG-conjugated DSPE (APRPG-PEG-DSPE) and PEG-conjugated DSPE (PEG-DSPE) were prepared as described previously.[11] StearoylAPRPG was synthesized according to the previous method.[3] Distearoylphosphatidylcholine (DSPC) was the product of Nippon Fine Chemical Co. (Hyogo, Japan). Cholesterol was purchased from Sigma (St. Louis, MO, U.S.A.). All other reagents used were the analytical grades.

Preparation of Liposomes Liposomes were prepared for the PET analysis as follows: DSPC and cholesterol with

* To whom correspondence should be addressed. e-mail: oku@u-shizuoka-ken.ac.jp

APRPG-PEG-DSPE or PEG-DSPE (10 : 5 : 1 as a molar ratio; APRPG-PEG-Lip or PEG-Lip, respectively), or DSPC and cholesterol without PEG conjugates (10 : 5 as a molar ratio; cont-Lip) were dissolved in chloroform and methanol, dried under reduced pressure, and stored *in vacuo* for at least 1 h. After hydration of the thin lipid films with 1.0 ml of 0.9 M glucose, the resulting liposomal solution was mixed 2.0 ml of [2-^{18}F]2-fluoro-2-deoxy-D-glucose ([2-^{18}F]FDG) solution and freeze-thawed for three cycles by liquid nitrogen in order to encapsulate the positron emitter-containing chemical into the liposomes: The osmolarity in the liposomal solution was similar to that under physiological condition. Then, the liposomes were extruded thrice through a polycarbonate membrane filter (100-nm pore size), washed by centrifugation at 180000×***g*** for 15 min after dilution with phosphate-buffered saline (PBS) to remove the untrapped [2-^{18}F]FDG, and finally resuspended in 1 ml of 0.3 M glucose.

To examine the intratumoral localization of liposomes in tumor syngrafts, liposomes were fluorescence-labeled with 1,1′-dioctadecyl-3,3,3′,3′-tetramethylindo-carbocyanine perchlorate ($DiIC_{18}$; Molecular Probes Inc., Eugene, OR, U.S.A.). DSPC, cholesterol and $DiIC_{18}$ with APRPG-PEG-DSPE or PEG-DSPE (20 : 10 : 1 : 2 as a molar ratio), or DSPC, cholesterol and $DiIC_{18}$ without PEG conjugates (20 : 10 : 1 as a molar ratio) were dissolved in chloroform and methanol, dried under reduced pressure, and stored *in vacuo* for at least 1 h. After hydration of the thin lipid film with 1.0 ml of 0.3 M glucose, the resulting liposomal solution was freeze-thawed for three cycles by liquid nitrogen. Then, the liposomes were extruded thrice through a polycarbonate membrane filter (100-nm pore size).

For therapeutic experiment, ADM-encapsulated liposomes were prepared by a modification of the remote-loading method as described previously,[12] and the encapsulation efficiency determined was more than 90% throughout the experiment. The concentration of ADM was determined by 484-nm absorbance.

PET Analysis of APRPG-PEG Modified Liposomes C26 NL-17 cells (1.0×10^6 cells/mouse) were injected subcutaneously into the posterior flank of 5-week-old BALB/c male mice (Japan SLC Inc., Shizuoka, Japan), and PET study was performed when the tumor size had become about 10 mm in diameter. Tumor-bearing mice weighing 23—26 g were injected into a tail vein with positron-labeled liposomes. The injected dose was 2 mmol as DSPC dosage, and about 0.5 MBq. The emission scan was started immediately after injection and performed for 120 min with an animal PET camera (Hamamatsu Photonics K.K., SHR-7700) having an effective slice aperture of 3.6 mm. Transmission scans were obtained by use of an 18.5 MBq ^{68}Ga/Ga ring source for attenuation correction before the liposomal injection. The radioactivity in the form of coincident gamma photons was measured and converted to Bq/cm^3 of tissue volume by calibration after correction for decay and attenuation. A time activity curve was obtained from the mean pixel radioactivity in the region of interest (ROI) of the PET images.

Histochemical Analysis of Liposomal Distribution in Tumor Syngrafts C26 NL-17 cells (1.0×10^6 cells/mouse) were inoculated as described above. $DiIC_{18}$-labeled liposomes were administered *via* a tail vein of C26 NL-17-bearing mice when the tumor sizes had reached about 10 mm. Two hours after the injection of liposomes, mice were sacrificed under anesthesia with diethyl ether, and the tumor was dissected. Solid tumors were embedded in optimal cutting temperature compound (Sakura Finetechnochemical Co., Ltd., Tokyo, Japan) and frozen at −80 °C. Five-micrometer tumor sections were prepared by using cryostatic microtome (HM 505E, Microm, Walldorf, Germany), mounted on MAS coated slides (MATSUNAMI GLASS Ind., Ltd., Japan), and air-dried for 1 h. The tissue sections were fixed in acetone for 10 min at room temperature, washed twice with PBS (5 min each time), and incubated with protein-blocking solution containing 1% bovine serum albumin in PBS for 10 min at room temperature. Then, the samples were incubated with an appropriately diluted (1 : 100) biotinylated anti-mouse CD31 rat monoclonal antibody (Becton Dickinson Lab., Franklin Lakes, NJ, U.S.A.) for 18 h at 4 °C. After the sections were rinsed three times (2 min each time) with PBS, they were incubated with streptavidin-FITC conjugates (Molecular Probes Inc., Eugene, OR, U.S.A.) for 30 min at room temperature in a humid chamber. Samples were washed twice with PBS (2 min each time). Finally, sections were counterstained and mounted with Perma Fluor Aqueous Mounting Medium (Thermo Shandon, Pittsburgh, PA, U.S.A.). These sections were fluorescently observed by using microscopic LSM system (Carl Zeiss Co., Ltd.): Endothelial cells were identified as green fluorescence and liposomes were detected as red.

Therapeutic Experiment C26 NL-17 cells (1.0×10^6 cells/mouse) were inoculated as described above. Liposomes encapsulating ADM or 0.3 M glucose solution were administered intravenously into C26 NL-17-bearing mice at day 11, 14, and 17 after the inoculation of tumor cells: The treatment was started when the tumor volumes became about 0.1 cm^3. The injected dose of ADM in each administration was 10 mg/kg (about 0.045 mmol/kg liposomal dose as DSPC in liposomal formulations). The size of the tumor and body weight of each mouse were monitored. Two bisecting diameters of each tumor were measured with slide calipers to determine the tumor volume and calculation was performed using the formula $0.4\times(a\times b^2)$, where a is the largest and b is the smallest diameter.

Statistical Analysis Differences in a group were evaluated by Student's t-test.

RESULTS

***In Vivo* Trafficking of [2-^{18}F]FDG-Labeled Liposomes Imaged by PET** We examined *in vivo* behavior of liposomes visually by use of PET. A PET study allows us to analyze real time distribution change of liposomes under non-invasive conditions. Liposomes prelabeled with [2-^{18}F]FDG were injected into C26 NL-17-bearing mice, and PET analysis was performed. PET images (Fig. 1a) and the time activity curves of liposomal ^{18}F (Fig. 2a) in the tumor indicated that APRPG-PEG-coated and PEG-modified liposomes highly accumulated in the tumor immediately after the injection, and this high accumulation was sustained for at least 120 min during PET scanning. The PET study also showed that APRPG-PEG-Lip and PEG-Lip tended to avoid RES trapping (Figs. 1b, c, Figs. 2b, c) consistent with previous observation.[13] In contrast to PEG-modified liposomes, cont-Lip tended to accumulate in the liver and spleen. These results

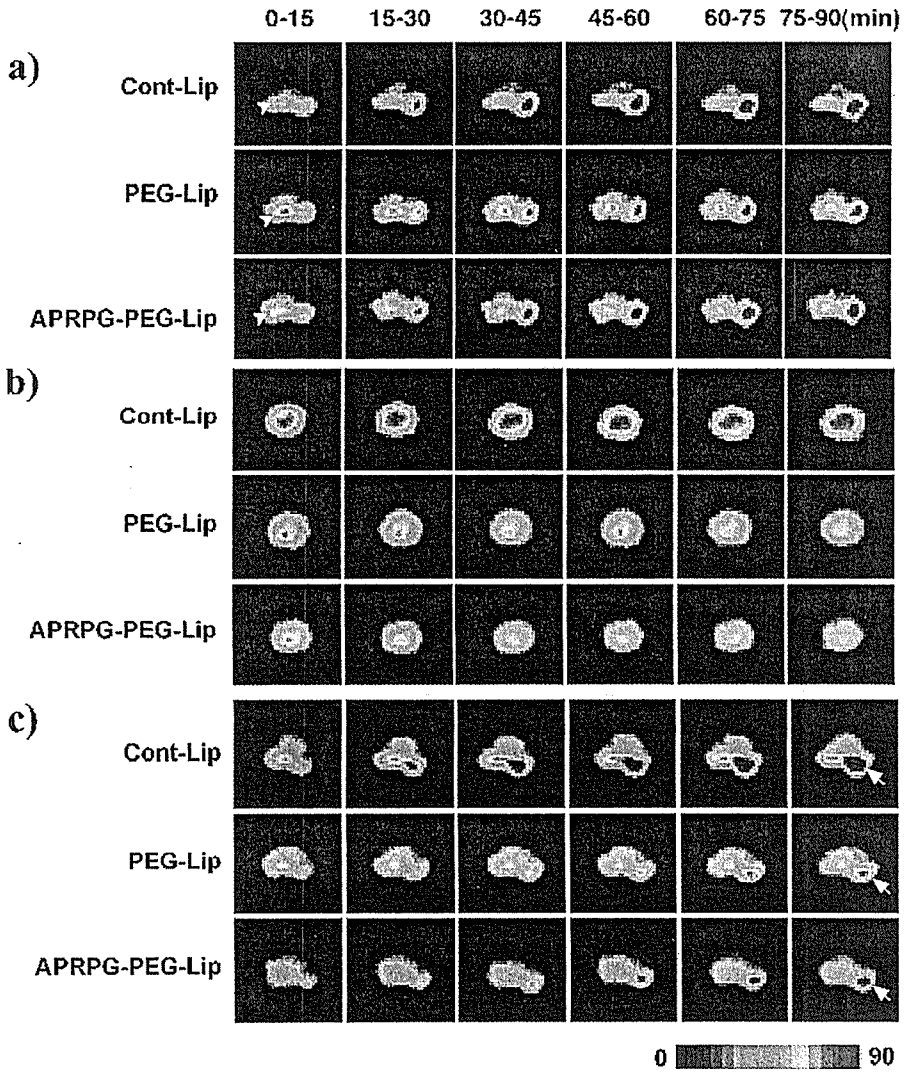

Fig. 1. PET Images of [2-^{18}F]FDG-Labeled Liposomal Distribution

Liposome composed of DSPC and cholesterol (upper panel), with DSPE-PEG (middle panel) or with DSPE-PEG-APRPG (lower panel) was prepared at a molar ratio of 10 : 5 : 1 in the presence of [2-^{18}F]FDG and extruded through 100-nm pores as described in Section 2. Gradation was corrected to be comparable in three groups. PET images show the accumulation of liposomes in the tumor (a), liver (b), or spleen (c) during every 15 min after injection. Coronal images of the tumor in each mouse are shown. Arrowheads indicate a location of the tumor. Arrows indicate that of the spleen. A separate experiment in the same procedure was performed and the similar results were obtained. Gradation bar indicates signal intensity.

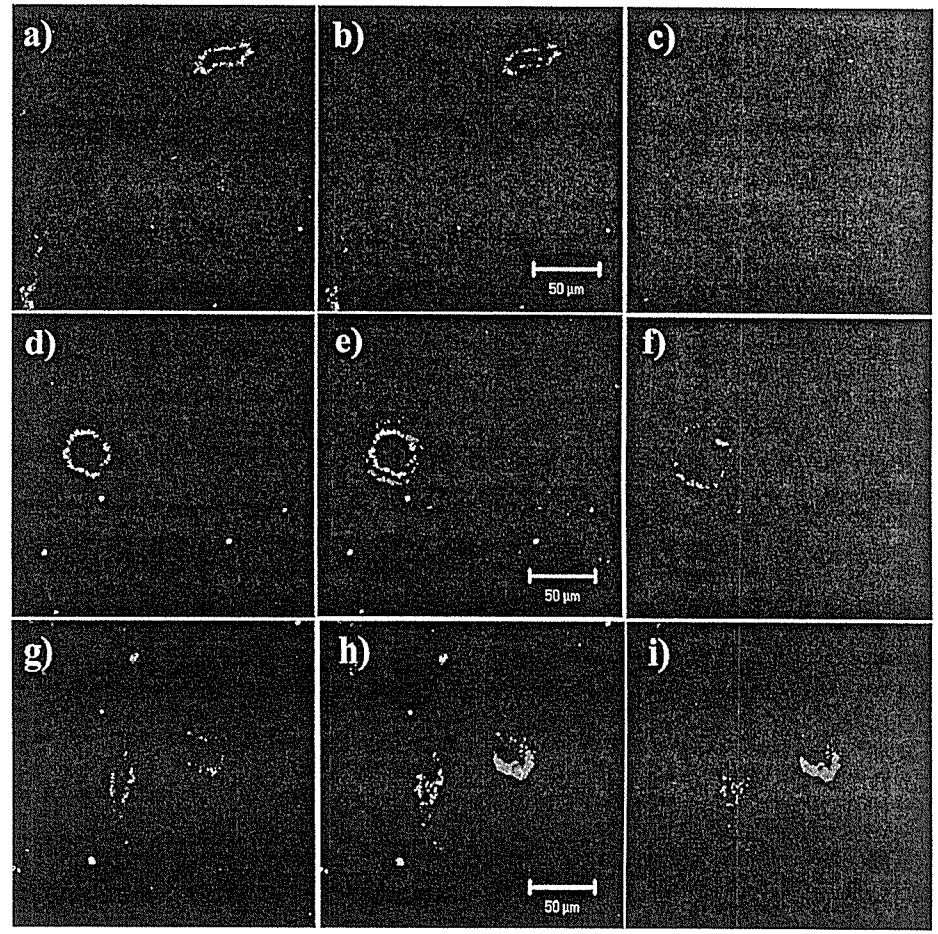

Fig. 3. Intratumoral Localization of DiIC$_{18}$-Labeled Liposomes after Injection

C26 NL-17-bearing mice were injected with Cont-Lip (a—c), PEG-Lip (d—f) or APRPG-PEG-Lip (g—i) labeled with DiIC$_{18}$ (c, f and i as red images) *via* tail vein on day 20 after tumor implantation. At 2 h after injection, each tumor was dissected and prepared for frozen-section. Micrographs derived from the image of CD31-staining vessels (a, d and g as green images). Panels b, e and h show the merged images of liposomal distribution and immunostaining for CD31, respectively. Yellow portions indicate localization of liposomes at the site of vascular endothelial cells. Separate experiments in the same procedure were performed and the similar results were obtained.

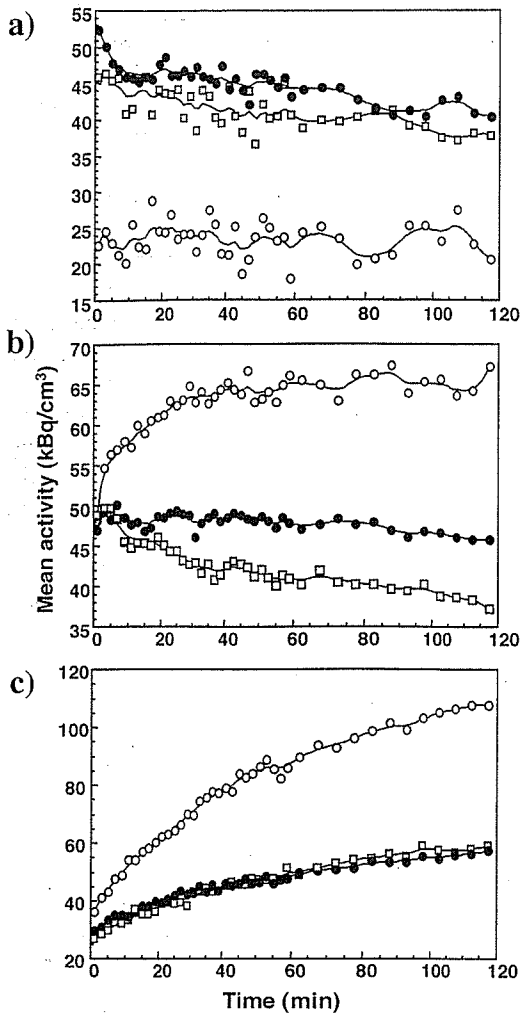

Fig. 2. Time-Dependent Accumulation of [2-^{18}F]FDG-Labeled Liposomes in Various Organs

Time–activity curves of ^{18}F in tumor (a), liver (b) and spleen (c) were obtained from the mean pixel radioactivity in ROI of the images shown in Fig. 1. C26 NL-17 carcinoma-bearing mice were injected with [2-^{18}F]FDG-labeled Cont-Lip (open circle), PEG-Lip (closed circle) or APRPG-PEG-Lip (open square).

were confirmed by the actual ^{18}F accumulation in the tumor, liver and spleen dissected from the mice after PET scanning (data not shown).

Intratumoral Distribution of APRPG-PEG-Modified Liposomes C26 NL-17-bearing mice were given a single i.v. dose of APRPG-PEG-Lip, PEG-Lip or Cont-Lip labeled with $DiIC_{18}$, and the mice were euthanized with diethylether anesthesia. Angiogenic endothelial cells in frozen sections of tumor organs were stained by immunohistochemical techniques and liposomal distribution in them was observed under confocal laser scanning microscopy. As shown in Figs. 3a—c, only a small amount of red fluorescence was observed, and some of them were surrounded with green fluorescence when cont-Lip was injected. On the contrary, red fluorescence was widely observed outside of green fluorescence in Figs. 3d—f, suggesting that PEG-Lip extravasated from tumor angiogenic vessels and accumulated in the tumor tissue. Interestingly, fluorescence of APRPG-PEG-Lip was colocalized with CD31-staining (Figs. 3g—i), suggesting that APRPG-PEG-Lip associated with angiogenic endothelial cells.

Table 1. Therapeutic Efficacy of APRPG-PEG-Modified Liposome Encapsulating ADM on Tumor-Bearing Mice

Treatment	Tumor volume (cm^3)	Growth inhibition (%)	Mean survival (d)
Control	3.28±0.52	—	50.3±6.0
APRPG-LipADM	1.38±0.69	57.8	55.5±7.8
PEG-LipADM	1.10±0.47	66.3	61.3±9.0
APRPG-PEG-LipADM	0.59±0.32[a)]	82.1	70.0±10.3[b)]

a) Significantly different from control ($p<0.001$), APRPG-LipADM ($p<0.05$) and PEG-LipADM ($p<0.05$). *b*) Significantly different from control ($p<0.001$) and APRPG-LipADM ($p<0.05$). C26 NL-17-bearing BALB/c mice ($n=6$) were injected i.v. with 0.3 M glucose (control), APRPG-LipADM, PEG-LipADM, or APRPG-PEG-LipADM for three times at day 11, 14 and 17 after the tumor implantation. Injected solutions of liposomal ADM were adjusted to 10 mg/kg as ADM concentration in each administration. The size change of the tumor at day 27 and the survival time of tumor-bearing mice are shown.

Therapeutic Efficacy of APRPG-PEG-Lip Encapsulating ADM Finally, therapeutic experiment was performed in a similar manner to that in a previous report[13] except that the effect of APRPG-modified non-pegylated liposomes was examined as well as that of pegylated liposomes at the present study: The liposomes encapsulating ADM (10 mg/kg as ADM in each administration) were injected thrice into C26 NL-17-bearing mice. As shown in Table 1, APRPG-PEG-LipADM suppressed tumor growth most efficiently compared with PEG-LipADM and APRPG-LipADM: The significant difference in tumor volume of APRPG-PEG-LipADM-treated group from that of the control ($p<0.001$), APRPG-LipADM-treated ($p<0.05$), and PEG-LipADM-treated group ($p<0.05$) was observed. Additionally, the results of body weight change indicated that liposomalization suppressed severe side effects of the drug in consistent with the previous results[11] (data not shown). Corresponding to the tumor growth suppression, treatment with APRPG-PEG-LipADM, elongated the survival time of the mice.

DISCUSSION

In general, treatment with anti-cancer drugs accompanies severe side effects, since they have the strong cytotoxicity against not only tumor cells but also normal growing cells. In order to prevent from severe side effects of these drugs, liposomes are useful tools for the carrier of these drugs. It is known that PEG-modified liposomes prevent from phagocytosis by macrophage and opsonization since these liposomes have water layer on liposomal surface.[14] The feature of long-circulation causes the liposomal accumulation in tumor tissues because angiogenic vasculature in tumor tissue is quite leaky and macromolecules are easily accumulate in the interstitial spaces of the tumor due to EPR effect.[8,9] Besides passive targeting, active targeting of pegylated liposomes has been widely studied: The distal end of PEG on liposomal surface is modified with various kinds of molecules (for example antibodies, Fab' fragments or other ligands) in order to enhance the affinity for targeted cell surface.[15] However, when these liposomes are targeted at tumor cells, passive accumulation of liposomes by EPR effect is prerequisite for active binding of the drug carrier to the target molecules. This uncertainty may affect targeting efficacy and subsequent therapeutic effect.

Correspondingly, we have developed a novel modality of

cancer treatment, antineovascular therapy, by use of angiogenic vasculature-targeting peptide, APRPG.[3,4] These 5-mer peptide-modified liposomes tend to accumulate to tumor tissue through specific binding to neovascular endothelial cells. Furthermore, APRPG-modified ADM-encapsulated liposomes significantly suppressed tumor growth.[3] When the endothelial cell surface molecules are targeted, extravasation of liposome from bloodstream to tumor parenchyma may not be required because angiogenic endothelial cells ordinarily border to bloodstream. We previously tried to endow APRPG-LipADM with long-circulating character for enhancing the targeting ability of the drug carrier to angiogenic vessels, and observed that APRPG-LipADM was quite effective for tumor growth suppression.[12] Since it is not clear that the mechanism of the enhanced therapeutic efficacy is based on the damage of angiogenic endothelial cells by ADM encapsulated in APRPG-PEG-Lip, we examined *in vivo* trafficking and intratumoral distribution of APRPG-PEG-Lip in the present study.

The results of PET study indicate that PEG-coated liposomes, despite conjugating with APRPG peptide, avoided to be trapped by RES such as liver and spleen, and tended to accumulate to tumor more than non-modified one. However, the *in vivo* behavior and tumor accumulation of APRPG-PEG-Lip was almost the same as that of PEG-Lip. Therefore, we examined the liposomal localization in tumor tissues by use of fluorescence-labeled liposomes. As shown in Fig. 3, PEG-Lip extravasated through angiogenic vasculature and accumulated in the interstitial space of tumor tissues due to EPR effect. On the contrary, APRPG-PEG-Lip associated to angiogenic endothelial cells due to active targeting by APRPG peptide attached to liposomal surface, although it is unclear whether these liposomes only bound to the endothelial cells or they were internalized. Since peptides containing some basic amino acids such as HIV Tat peptide are known to electrically interact with plasma membrane and to be internalized,[16] it is possible that APRPG-PEG-Lip similarly interacted with the cells. However, we believe that APRPG-PEG-Lip interacted through a certain molecule on the cell surface, since the presence of excess peptide inhibited the binding of APRPG-Lip to VEGF-stimulated endothelial cells.[3]

Concerning the difference in intratumoral distribution between PEG-Lip and APRPG-PEG-Lip, apparent therapeutic efficacy of APRPG-PEG-LipADM shown in Table 1 would be explained that the damaging of angiogenic endothelial cells is effective for tumor growth suppression. This evidence suggests the importance of accessibility of liposomal anticancer drugs to angiogenic endothelial cells on therapeutic efficacy, rather than the total accumulation amount of them in tumor tissue.

Recently, Schiffelers *et al.*[17] and Pastorino *et al.*[18] reported ANET in similar idea to that of the present study by using targeting peptide-modified long-circulating liposomes encapsulating ADM: RGD peptide which might bind to integrin $\alpha_v\beta_3$ on the angiogenic endothelial cells or NGR peptide which targeted aminopeptidase N, a marker of these cells, was used as targeting molecules, respectively. As targeting molecules, short peptide fragments are very useful and attractive because of their ease of identification and production without heavy immunogenicity.

In this study, we compared the characteristics between APRPG-PEG-Lip and PEG-Lip, and demonstrated therapeutic potential of APRPG-PEG-LipADM in cancer chemotherapy. We concluded that this efficacy was partly referred from the active targeting efficiency of APRPG-PEG-Lip. Additionally, APRPG-PEG-Lip keeps long-circulating property, which enhances the opportunity of liposomal binding to angiogenic endothelial cells. Consequently, it would be expected that APRPG-PEG-Lip could effectively deliver anticancer agents for anti-neovascular therapy, or anti-angiogenic agents for tumor dormancy therapy. Furthermore, it is considered that APRPG-PEG may be useful for human cancer treatment, since APRPG-PEG-Lip have affinity for VEGF-stimulated human umbilical vein endothelial cells.[13]

REFERENCES

1) Folkman J., D'Amore P. A., *Cell*, **87**, 1153—1155 (1996).
2) O'Reilly M. S., Holmgren L., Chen C., Folkman J., *Nat. Med.*, **2**, 689—692 (1996).
3) Oku N., Asai T., Watanabe K., Kuromi K., Nagatsuka M., Kurohane K., Kikkawa H., Ogino K., Tanaka M., Ishikawa D., Tsukada H., Momose M., Nakayama J., Taki T., *Oncogene*, **21**, 2662—2669 (2002).
4) Asai T., Shimizu K., Kondo M., Kuromi K., Watanabe K., Ogino K., Taki T., Shuto S., Matsuda A., Oku N., *FEBS Lett.*, **520**, 167—170 (2002).
5) Shimizu K., Asai T., Fuse C., Sadzuka Y., Sonobe T., Ogino K., Taki T., Tanaka T., Oku N., *Int. J. Pharm.*, **296**, 133—141 (2005).
6) Sakakibara T., Chen F. A., Kida H., Kunieda K., Cuenca R. E., Martin F. J., Bankert R. B., *Cancer Res.*, **56**, 3743—3746 (1996).
7) Lasic D. D., *Nature* (London), **380**, 561—562 (1996).
8) Auguste D. T., Prud'homme R. K., Ahl P. L., Meers P., Kohn J., *Biochim. Biophys. Acta*, **1616**, 184—195 (2003).
9) Maeda H., Wu J., Sawa T., Matsumura Y., Hori K., *J. Control. Release*, **65**, 271—284 (2000).
10) Muggia F. M., *Clin. Cancer Res.*, **5**, 7—8 (1999).
11) Maeda N., Takeuchi Y., Takada M., Namba Y., Oku N., *Bioorg. Med. Chem. Lett.*, **14**, 1015—1017 (2004).
12) Maeda N., Takeuchi Y., Takada M., Sadzuka Y., Namba Y., Oku N., *J. Control. Release*, **100**, 41—52 (2004).
13) Oku N., *Adv. Drug Deliv. Rev.*, **37**, 53—61 (1999).
14) Oku N., *Adv. Drug Deliv. Rev.*, **40**, 63—73 (1999).
15) Allen T. M., *Nat. Rev. Cancer*, **2**, 750—763 (2002).
16) Fittipaldi A., Giacca M., *Adv. Drug Deliv. Rev.*, **57**, 597—608 (2005).
17) Schiffelers R. M., Koning G. A., ten Hagen T. L., Fens M. H., Schraa A. J., Janssen A. P., Kok R. J., Molema G., Storm G., *J. Control. Release*, **91**, 115—122 (2003).
18) Pastorino F., Brignole C., Marimpietri D., Cilli M., Gambini C., Ribatti D., Longhi R., Allen T. M., Corti A., Ponzoni M., *Cancer Res.*, **63**, 7400—7409 (2003).

Available online at www.sciencedirect.com
SCIENCE DIRECT
Cancer Letters 241 (2006) 42–48
CANCER Letters
www.elsevier.com/locate/canlet

The phototoxicity of photofrin was enhanced by PEGylated liposome in vitro

Yasuyuki Sadzuka [a,*], Koji Tokutomi [a], Fumiaki Iwasaki [a], Ikumi Sugiyama [a], Toru Hirano [b], Hiroyuki Konno [c], Naoto Oku [a], Takashi Sonobe [a]

[a] *School of Pharmaceutical Sciences, University of Shizuoka, 52-1 Yada, Shizuoka 422-8526, Japan*
[b] *Photon Medical Research Center, Hamamatsu University School of Medicine 1-20-1 Handayama, Hamamatsu, Shizuoka 431-3192, Japan*
[c] *Second Department of Surgery II, Hamamatsu University School of Medicine 1-20-1 Handayama, Hamamatsu, Shizuoka 431-3192, Japan*

Received 20 January 2005; received in revised form 8 September 2005; accepted 6 October 2005

Abstract

In recent years, photodynamic therapy (PDT) with a photosensitizer and laser has been given attention, especially for the treatment of superficial cancers, such as lung, gastric, bladder and cervical cancer. In this study, in order to enhance the efficacy of PDT, photofrin liposome (PF-Lip) was prepared with dimyristoylphosphatidylcholine, dimyristoylphosphatidylglycerol and cholesterol. Polyethyleneglycol modified photofrin liposome (PF-PEG-Lip) was prepared by modification of PF-Lip with monomethoxypolyethyleneglycol-2.3-dimyristoylglycerol. PF-Lip and PF-PEG-Lip entrapped with photofrin with 81.0±5.9 and 81.2±9.2%, respectively. The particle size of each liposome was 114.3±5.7 nm (PF-Lip) and 118±3.5 nm (PF-PEG-Lip), respectively. It was suggested that PEGylated liposomes has no effect on the trapping ratio of PF and particle size. Phototoxicity was enhanced by liposomalization, especially PEG-modification. However, PF-PEG-Lip inhibited the uptake of photofrin into tumor cells. The amount of singlet oxygen from photofrin solution (PF-sol) and each liposome was PF-PEG-Lip≒PF-Lip>PF-sol. The photofrin release revel of PF-PEG-Lip was lower than that of PF-Lip.

In conclusion, the phototoxicity of PF-PEG-Lip was significantly higher than that of PF-sol or PF-Lip. It is expected that formation of a fixed aqueous layer on the liposome membrane by PEGylation physically changed it into the stable state of PF-PEG-Lip.

Keywords: Liposome; Photodynamic therapy (PDT); Photofrin; Singlet oxygen

1. Introduction

Photodynamic therapy (PDT), which involves photosensitizer and laser has been established as a potent and less invasive treatment for various malignant tumors [1–4]. photofrin, a hematoporphyrin derivative activated with red light of 630 nm, has been approved and commercialized in European and Asian countries, as well as in North America [5]. Especially in Japan, PDT with photofrin has been supported by government medical insurance since 1996. The antitumor effect of PDT is triggered by the singlet oxygen generated from the photosensitizer under laser irradiation [6–8].

Abbreviations PDT, photodynamic therapy; PF-Lip, photofrin liposome; PF-PEG-Lip, polyethyleneglycol modified photofrin liposome; PF-sol, photofrin solution; DMPC, L-α-dimyristoylphosphatidylcholine; DMPG, L-α-dimyristoylphosphatidyl-DL-glycerol; PEG-DMG, 1-monomethoxypolyethyleneglycol-2,3-dimyristoylglycerol; PBS, phosphate-buffered saline; T_c, transition temperature; EDL, excimer dye laser; PMT, photomultiplier tube; EPR, enhanced permeability and retention.

* Corresponding author. Tel.: +81 54 264 5610; fax: +81 54 264 5615.
E-mail address: sadzuka@u-shizuoka-ken.ac.jp (Y. Sadzuka).

0304-3835/$ - see front matter © 2005 Elsevier Ireland Ltd. All rights reserved.
doi:10.1016/j.canlet.2005.10.024

The difference in concentration of the photosensitizer makes it possible to damage tumor tissue with less damage to the surrounding normal tissues [9].

Liposomes have been applied as a carrier in various fields to modify the distribution of the chemical agents [10,11]. This strategy is based on the premise that liposomes are preferentially absorbed by sites of disease such as tumors. It is known that polyethyleneglycol (PEG)-modification of liposomes avoids trapping liposomes by the reticuloendothelial system (RES), as a result, this increases the distribution of liposomes in the tumor [12–14]. It is reported that liposomalization of the photosensitizer enhanced the effect of PDT based on its tumor accumulation [15]. Liposomal benzoporphyrin derivative monoacid ring A (BPD-MA, verteporfin) shows an enhanced therapeutic effect against Meth A sarcoma in nude mice, and liposomal 2,3-dihydro-5,15-di(3,5-dihydroxyphenyl)-porphyrin (SIM01) shows an enhanced effect against HT29 human adenocarcinoma in nude mice [16]. Furthermore, liposomal photofrin enhanced therapeutic efficacy of PDT against 9L gliosarcoma, U87 human glioma and human gastric cancer [17–19]. However, there are few reports on the phototoxicity and the effect of active oxygen generation by liposomalization of photosensitizer and its PEGylation [20].

In this study, we investigated the liposomalization of photofrin, and evaluated the cytotoxicity of liposomal photofrin in vitro with M5076 ovarian sarcoma. Furthermore, we attempted to make clear the mechanism of the enhancement of PDT through the measurement of singlet oxygen.

2. Material and method

2.1. Materials

Photofrin, porfimer sodium injection, was purchased from Nippon Lederly Co., Ltd (Tokyo, Japan). L-α-Dimyristoylphosphatidylcholine (DMPC) and L-α-dimyristoylphosphatidyl-DL-glycerol (DMPG) were kindly donated by Nippon Oil and Fat Co., Ltd (Tokyo, Japan). 1-Monomethoxypolyethylene-glycol-2,3-dimyristoylglycerol (PEG-DMG) was kindly provided by Nippon Oil and Fat Co., Ltd. RPMI-1640 medium was purchased from Nissui Pharmaceutical Co., Ltd (Tokyo, Japan).

2.2. Tumor

An M5076 ovarian sarcoma was maintained through intraperitoneal passage and implanted on the backs of male C57BL/6 mice obtained from Japan SLC, Inc. (Hamamatsu, Japan). The animals were housed in a room maintained at 25 ± 1 °C and 55 ± 5% relative humidity, and were given free access to regular food pellets and water.

2.3. Preparation of liposomes

All liposomes were prepared according to a modification of the method of Bangham et al. [21].

DMPC/cholesterol/DMPG (100/100/60 μmol) and 30 mg of photofrin were dissolved in a chloroform/-methanol mixture (4/1, v/v). The chloroform and methanol were evaporated under a stream of nitrogen gas. The thin lipid film was placed in a desiccator, which was evacuated, and then the lipid film was hydrated with 8.0 ml of phosphate-buffered saline (PBS(−)) in a water bath at 65 °C for 10 min. The suspension was sonicated for 20 min above the phase transition temperature (T_c) with nitrogen gas bubbling. The liposome suspension was extruded through two stacked polycarbonate membrane filters with 0.2 μm pores, and then passed five times through polycarbonate membrane filters with 0.1 μm pores at above the T_c, to obtain a homogeneously-sized liposome suspension. PF-Lip was prepared by adding 2.0 ml of PBS(−) to this suspension. On the other hand, PF-PEG-Lip was prepared by adding 2.0 ml of PBS(−) containing 15 μmol PEG-DMG, and then sonicated for 5 min. Each liposome suspension was dialyzed against PBS(−) at 4 °C for 16 h to remove untrapped photofrin. The particle sizes and zeta-potentials of the liposomes were measured with an electophoretic light scattering apparatus (ELS 8000; Otsuka Electronics, Co., Ltd Osaka, Japan). Entrapment efficiency of photofrin in liposome was measured to the following. Liposomes encapsulating photofrin were mixed for 30 s with lactate buffer (pH 4.0) and chloroform/isopropanol (1/1, v/v), and then centrifugated at 1200*g* for 15 min. Photofrin in the organic phase was calculated with a fluorescence spectrophotometer (Hitachi F2000; Hitachi Ltd, Tokyo), at an excitation wavelength of 405 nm and an emission wavelength of 630 nm.

2.4. PDT in vitro

M5076 ovarian sarcoma cells (1×10^5 cells/ml) were suspended in RPMI 1640 medium containing 10% FBS in a 35-mm cell culture dish. This cell suspension containing PF-sol, PF-Lip or PF-PEG-Lip (PF concentration, 2, 5 or 10 μg/ml) was incubated for 60 min at 37 °C. Each cell suspension was exposed to

laser light of 630 nm with 2 J/cm^2 of fluence (0.1 W, 192 s) and then incubated for 24 h at 37 °C. Cell survival was determined by 4-[3-(2-methoxy-4-nitrophenyl)-2-(4-nitrophenyl)-2H-5-tetrazolio]-1,3-benzene disulfonate sodium salt (WST-8) using a commercially available kit (TetraColor ONE cell proliferation assay system; Seikagaku Co., Tokyo, Japan). Each cell suspension was transferred to a microtube and centrifuged at 300*g* for 5 min. The cells were washed and resuspended in RPMI-1640 medium. TetraColor ONE (50 μl) was added to each cell suspension and incubated for 3 h at 37 °C. Each cell suspension was centrifuged at 300*g* for 5 min, and absorbances at 492 and 630 nm of the supernantant were measured using a microplate reader. Absobance (A492-A630) correlates with the number of living cells.

2.5. Uptake of photofrin into tumor cells

M5076 ovarian sarcoma cells (1×10^6 cells/animal) were intraperitonally transplanted into male C57BL/6 mice. Ascites fluid was collected on the 14th day after transplantation. The M5076 ovarian sarcoma cells were washed twice and then resuspended (5×10^6 cells/ml) in RPMI-1640 medium containing 10% FBS.

The cell suspension containing PF-sol, PF-Lip or PF-PEG-Lip (photofrin concentration, 10 μg/ml) was incubated at 37 °C for 90 min. For determination of the time course of the intracellular drug concentration, aliquots of the cell suspension were removed at intervals. Each aliquot was cooled on ice and then centrifuged at 150*g* for 3 min. The cells were washed and resuspended in 1.0 ml of ice-cold saline, mixed for 30 s with 3.0 ml THF and 0.5 g NaCl, and then centrifuged at 1200*g* for 15 min. The concentration of the photofrin in the organic phase was determined as described above.

2.6. Measurement of singlet oxygen

For the sample, PF-sol, PF-Lip, PF-PEG-Lip and photofrin were dissolved in CH_2Cl_2/EtOH (9/1, v/v). Each sample was diluted with PBS(−) or CH_2Cl_2/EtOH (9/1, v/v), in order to achieve 0.5 as the absorption at 630 nm.

A quartz cuvette filled with each sample was irradiated by laser light (630 nm, 20 mW) generated excimer dye laser (EDL). Reflected or scattered light from the cuvette was guided to the detection system (Fig. 1) which contained a spectroscope, a single channel detector PMT (Hamamatsu Photonics, R5509-42) or a multichannel detector (Hamamatsu Photonics, NIR-PII) and a photon-counter. To separate the 1270 nm emission from the photosensitizer fluorescence, detectors were gated with a delay time from the onset of the laser pulse irradiation and a gate time width, synchronized with laser the pulses. In this study, the energy generated at 1260–1280 nm was detected by the system.

2.7. Determination of the release of PF from liposomes

PF-Lip and PF-PEG-Lip were incubated in 50% FBS/PBS(−) for 3 h at 37 °C. The concentration of

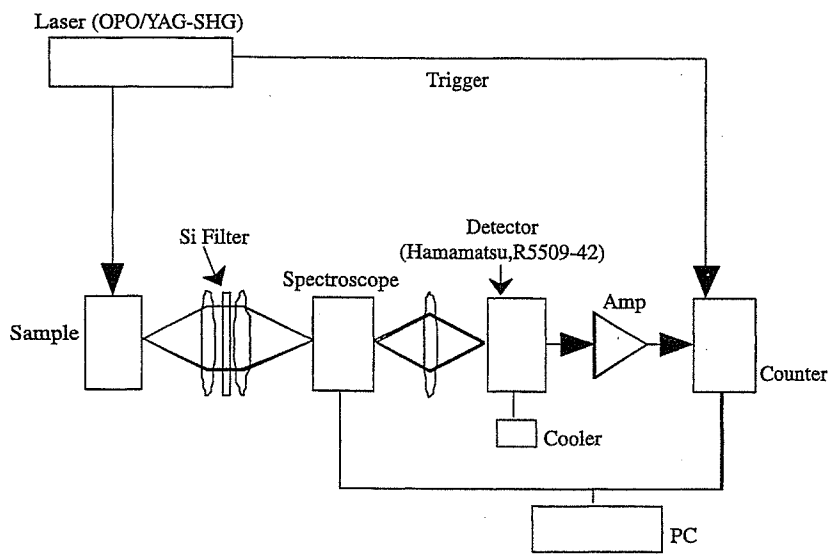

Fig. 1. Detection system of 1270 nm emission from the singlet oxygen.

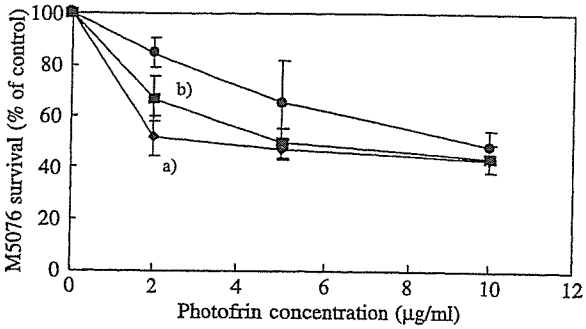

Fig. 2. Phototoxicity of photofrin against M5076 ovarian Sarcoma by PDT. M5076 ovarian sarcoma cell suspension containing PF-sol (●), PF-Lip (■) or PF-PEG-Lip (◆) (photofrin dose 2, 5 or 10 μg/ml) was incubated for 1 h at 37 °C. Each sample was exposed to laser light (630 nm, 2 J/cm^2), and was then incubated for 24 h at 37 °C. Survival ratio of M5076 ovarian sarcoma cells was determined by WST-8 assay. Data are presented as mean±SD (n=4). Significant differences from PF-sol are indicated by (a) $P<0.05$ and (b) $P<0.01$.

photofrin was 1.0 μg/ml at both samples. After a predetermined time, each liposome suspension was cooled on ice and then centrifuged at 180,000g (4 °C) for 60 min. The photofrin concentration in the supernatant was determined as described above. The leakage of photofrin from the liposomes was calculated from the photofrin concentration in the supernantant before and after being centrifuged.

2.8. Statistical analysis

Statistical analysis was carried out by Student's t-test and ANOVA.

3. Results

3.1. Physicochemical characteristics of photofrin liposomes

PF-Lip and PF-PEG-Lip entrapped photofrin with 81.0±5.9 and 81.2±9.2% efficiency, respectively, suggesting that photofrin was stably incorporated into the lipid bilayer. The particle size of each liposome was 114.3±5.7 nm (PF-Lip) and 118.4±3.5 nm (PF-PEG-Lip). It was suggested that PEGylated liposomes has no effect on these particle sizes. Because of the negative charge of DMPG in the lipid bilayer, the zeta-potential of PF-Lip was −38.2±9.9 mV. On the other hand, the zeta-potential of PF-PEG-Lip was −5.3±9.7 mV, smaller than that of PF-Lip, since PEG formed water layer, fixed aqueous layers, on the surface of the liposomes.

3.2. PDT in vitro

M5076 ovarian sarcoma cell suspension (1.0×10^5 cells/ml) containing PF-sol or PF-Lip or PF-PEG-Lip was incubated for 1 h at 37 °C. Each sample was exposed to laser light of 630 nm with 2 J/cm^2. At every concentration, the photofrin induced cytotoxic effect was PF-sol<PF-Lip<PF-PEG-Lip, suggesting that photosensitizer induced toxicity was enhanced by liposomalization, especially PEGylation. At the point of 2 μg/ml photofrin, survival ratios in PF-Lip and PF-PEG-Lip group significantly decreased ($P<0.05$ and $P<0.01$, respectively), compared to that in PF-sol group (Fig. 2).

3.3. Uptake of photofrin into tumor cells

In the determined period, the intercellular photofrin level was PF-Lip>PF-sol>PF-PEG-Lip. Especially at 60 min, a significant difference ($P<0.01$) was observed (Fig. 3, PF-Lip: 2.45±0.31, PF-sol: 1.20±0.11, PF-PEG-Lip: 0.61±0.04 μg/10^7 cells).

3.4. Measurement of singlet oxygen

A laser beam of 630 nm and 20 mW irradiated PF-sol, PF-Lip, PF-PEG-Lip and photofrin in 90% CH_2Cl_2. Then, the emission at 1260–1280 nm was detected by the system, and accumulated these photon counts. As a result, it was suggested that the amount of singlet oxygen generated by irradiation was PF-PEG-Lip≒PF-Lip>PF-sol (Fig. 4, Table 1). Futhermore, photofrin in 90% CH_2Cl_2 generated more singlet oxygen than PF-PEG-Lip. There were reproducibility about this results.

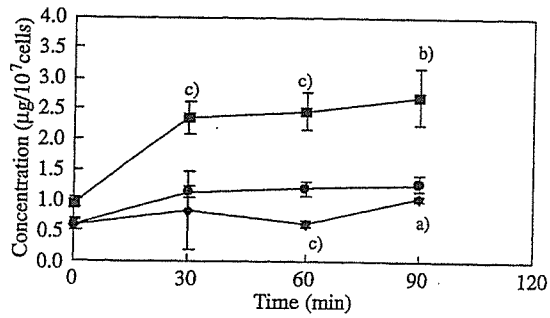

Fig. 3. Effect of liposomalization on photofrin uptake in M5076 ovarian sarcoma. Tumor cell suspension containing PF-sol (●), PF-Lip (■) or PF-PEG-Lip (◆) (photofrin dose 10 mg/kg) was incubated at 37 °C. Data are presented as mean±SD (n=4). Significant differences from PF-sol are indicated by (a) $P<0.05$, (b) $P<0.01$ and (c) $P<0.005$.

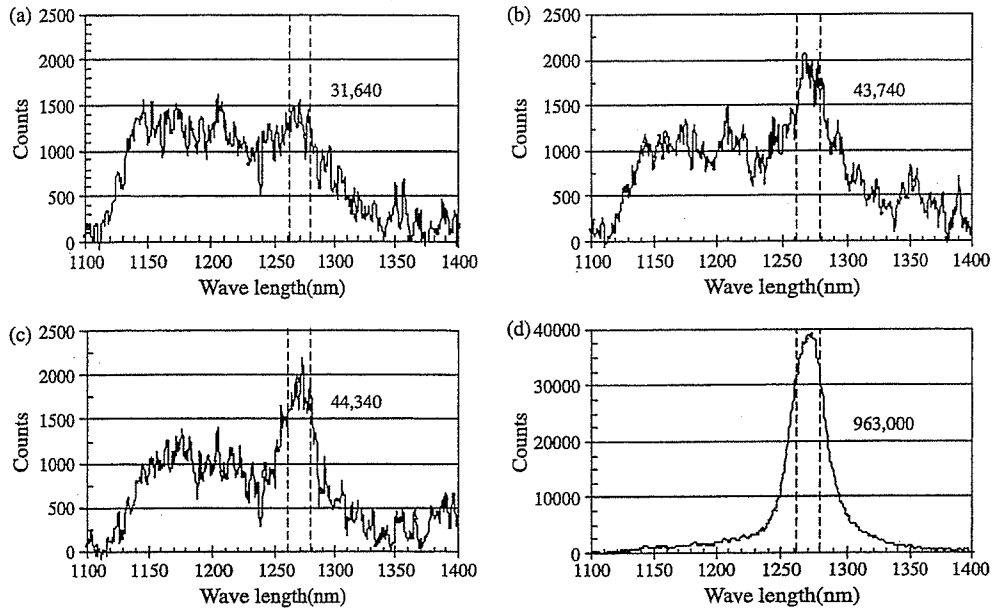

Fig. 4. Emission of 1270 nm from photofrin. Each sample was exposed to laser light (630 nm, 20 mW), and the generated singlet oxygen was detected by PMT. (A) Photofrin in PBS, (B) PF-Lip in PBS, (C) PF-PEG-Lip in PBS, (D) photofrin in 90% CH_2Cl_2.

3.5. Determinaton of the release of photofrin from liposomes

The photofrin release from each liposome was examined by incubation at 37 °C in 50% FBS/-PBS(−). At the initial 60 min, 79.6 ± 5.4% of photofrin was released from PF-Lip; the remainder was released by 180 min (Fig. 5). On the other hand, only 60.6 ± 16.3% of photofrin was released by PF-PEG-Lip (Fig. 5). It was suggested that the release of photofrin was inhibited by PEG-modification.

4. Discussion

PDT has been considered to show favorably in the treatment of malignant tumors since both novel photosensitizers and laser systems have developed recently, and further development can be expected in the future. The cytotoxicity of PDT is caused by the photochemical reaction that occurs when the photosensitizer is exposed to the light of a specific wavelength. Several reports have demonstrated that liposomalization of the photosensitizer enhanced the efficiency of PDT based on high accumulation in the tumor [22–26]. We previously reported that liposomal photofrin enhanced therapeutic efficacy of photodynamic therapy. Furthermore, the phototoxicity and the effect of active oxygen generation by liposomalization of AlPcS4 and its PEGylation have been reported [27]. However, in the case of photofrin as clinical medicine, the improvement of therapeutic index are not examined sufficiently. Thus, we examined the usefulness of liposome as a drug carrier and other function.

Generally, it is considered that a lower trapped ratio is shown in case of liposomalization of the hydrophilic agent by the method of Bangham, since the volume proportion of the inner/outer compartment is very small when it is entrapped in the inner compartment. As photofrin is an acidic drug (pKa ≒ 5.8) and PBS(−) (pH 7.0) are used for hydration, the rate of the ionized form is about 94.1%, so photofrin is easily entrapped in inner compartment of the liposome. However, since the photofrin trapping ratio in both PF-Lip and PF-PEG-Lip was more than 80%, it was expected that photofrin was entrapped in the liposome membrane, too. Namely, it was suggested that photofrin existed in the liposome membrane and inner compartment.

Table 1
Generation ability of the singlet oxygen

	Absorption	Area under the photon count curve	Ratio
PF-sol	0.5	31,640	1.00
PF-Lip	0.5	43,740	1.38
PF-PEG-Lip	0.5	44,340	1.40
PF-in CH_2Cl_2	0.5	963,000	30.4

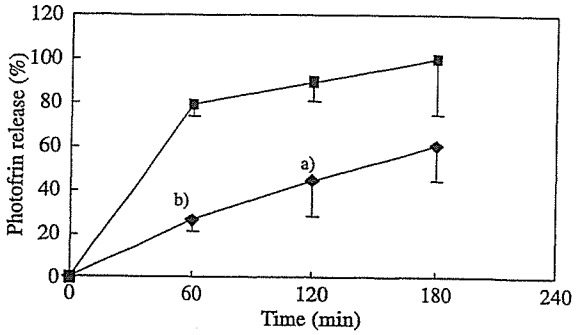

Fig. 5. Stability of liposomes containing photofrin. Photofrin release levels are expressed as a percentage of total photofrin in PF-Lip (■) or PF-PEG-Lip (♦). Each sample was incubated at 37 °C in 50% FBS. Data are presented as mean ± SD ($n=3$). Significant differences from PF-sol are indicated by (a) $P<0.01$ and (b) $P<0.001$.

We evaluated the survival ratio of M5076 ovarian sarcoma after PDT with PF-sol or each photofrin liposome. The survival of M5076 ovarian sarcoma was PF-sol > PF-Lip > PF-PEG-Lip (Fig. 2) and there were significant differences between each group. In contraction, on photofrin induced adverse reaction, we previously reported that dark toxicity of the formation used was not observed [28]. These results suggested that the phototoxicity of the photosensitizer was enhanced by liposomalization, especially by PEGylation.

Then, in order to clarify the enhanced effect of the PEGylation, we investigated the uptake of photofrin into tumor cells, ability to generate the singlet oxygen and the release of photofrin from the liposome. We evaluated the effect of liposomalization of photofrin on the uptake into M5076 ovarian sarcoma cells. As a result, the concentration of intracellular photofrin was the highest in PF-Lip group, whereas that of PF-PEG-Lip was lower than PF-sol (Fig. 3). These results suggested that the layer of PEG existed on the surface of the liposome membrane inhibits the binding of liposomes to cells, and thus prevents internalization of liposomes into the cells.

The photosensitizer loaded into the tumor cells generates singlet oxygen by laser irradiation, and thus necrosis is induced in the cells [5–8]. Namely, it is expected that the affinity of agent to tumor cell, and the ability to generate singlet oxygen is the most important factor of PDT therapy [7].

It is considered that the cytotoxicity of PDT is triggered by the singlet oxygen generated from the photosensitizer [6–8], and detection of the singlet oxygen is very important in understanding the mechanism of PDT. We measured the amount of singlet oxygen from PF-sol, PF-Lip, PF-PEG-Lip and PF in 90% CH_2Cl_2 in comparison to photofrin in aqueous solvent. On exposure to light of a specific wavelength, the photosensitizer is activated from its ground state S_0 to the excited state S_1. A part of the photosensitizer in the S_1 state transfers to the triplet state T_1 by way of intersystem crossing, and then the photosensitizer in the T_1 state transfers its energy to surrounding triplet oxygen ($^3O_2$), and causes the generation of active singlet oxygen ($^1O_2$). When the singlet oxygen decays to the triplet state, 1270 nm light is released. We detected this emission using a photon-counting method with a high sensitive single channel detector, photomultiplier tube (PMT) or a multichannel detector. The amount of singlet oxygen from photofrin was PF-PEG-Lip ≒ PF-Lip > PF-sol. It is known that singlet oxygen disappears immediately in aqueous solvents such as PBS(−), and their $T_{1/2}$ is prolonged in hydrophobic solvents such as CH_2Cl_2. It is known that singlet oxygen in aquenous solvents disappears rapidly. photofrin existed in liposome membrane as hydrophobic environment and the ability to generate singlet oxygen increased. It was suggested that the ability to generate singlet oxygen was influenced in the PDT by liposomalization and the PEGylated liposome.

The photofrin release from each liposome was PF-Lip > PF-PEG-Lip in 50%FBS/PBS(−) (Fig. 5). In particular, in PF-Lip, photofrin was released from the liposome during the incubation period. Since phase transition temperature of DMPC is 23 °C, PF-Lip may easily release photofrin by incubation at 37 °C. These results suggested that photofrin entrapped in the liposome membrane was not stable. Whereas, the PEGylated liposome inhibited the release of photofrin by about half. It was considered that formation of a fixed aqueous layer on the liposome membrane by PEGylation physically changed it into the stable state of PF-PEG-Lip. Due to this change, PF-PEG-Lip prolonged the photofrin retention time in its membrane. Namely, it was demonstrated that PF-PEG-Lip was effective for PDT in vitro.

Many previous reports have suggested that liposomalization of agents increases its accumulation in the tumor because of enhanced permeability and retention (EPR) effects [22–26]. Furthermore, it was known that the PEGylation was effective for the avoidance of RES trapping of liposomes. Therefore, PF-PEG-Lip is expected to produce a higher accumulation in the tumor than PF-Lip, and have a superior PDT effect in vivo, too.

In this study, we found the novel superiority of liposomalization on addition of function as the drug carrier in PDT. PEGylation of the liposomes prolonged

the retention time of the photosensitizer in the liposome membrane, thus showing significantly higher cytotoxicity. It is considered that this will make a great contribution to study of PDT.

References

[1] T. Hirano, The present condition of the laser for PDT, J. Jpn. Soc. Laser Surg. Med. 21 (2000) 129–135.

[2] K. Itou, T. Kano, S. Kobayashi, The photodynamic therapy over endoscope-early stomach cancer, Biotherapy 5 (1991) 546–551.

[3] H. Kato, H. Takahasi, T. Konaka, M. Ishii, T. Miura, The photodynamic therapy of lung cancer, Biotherapy 5 (1991) 536–545.

[4] H. Hisazumi, The photodynamic therapy in a urology department domain, J. Jpn. Soc. Laser Surg. Med. 8 (1987) 11–14.

[5] Wesley.M. Sharman, Cynthia.M. Allen, Johan.E. Van Lier, Photodynamic therapeutics: basic principles and clinical applications, Drug Discov. Today 4 (11) (1999) 507–717.

[6] Y.N. Konan, R. Gurny, E. Allemann, State of the art in the delivery of photosensitizers for photodynamic therapy, Photochem. Photobiol. 66 (2002) 89–106.

[7] M.C. DeRosa, R.J. Crutchley, Photosensitized singlet oxygen and its applications, Coord. Chem. Rev. 233–234 (2002) 351–371.

[8] R.D. Almeida, B.J. Manadas, A.P. Carvalho, C.B. Duarte, Intracellular signaling mechanisms in photodynamic therapy, Biochim. Biophys. Acta 1704 (2004) 59–86.

[9] D.A. Bellnier, T.J.A. Dougherty, Preliminary pharmacokinetic study of intravenous photofrin in patients, J. Clin. Laser Med. Surg. 14 (1996) 311–314.

[10] Y.M. Rustem, C. Dave, E. Mayhew, D. Papahadjopoulos, Role of liposome type and ruote of administration in the antitumor activity of liposome-entrapped 1-bate-D-arabinofuranosylcytosine against mouse L1210 Leukemia, Cancer Res. 39 (1979) 1390–1395.

[11] R.M. Abra, C.A. Hunt, D.T. Lau, Liposome disposition in vivo, J. Pharm. Sci. 73 (1984) 203–206.

[12] T. Yuda, Y. Pongpaibul, K. Maruyama, M. Iwatatsuru, Activity of amphipathic polyethylene glycol prolong the circulation time of liposomes, J. Pharm. Sci. Jpn 59 (1999) 32–42.

[13] A. Gobizon, D. Goren, A.T. Horowitz, D. Tzemach, A. Lossos, T. Siegal, Long-circulating liposomes for drug delivery in cancer therapy: a review of biodistribution studies in tumor-bearing animals, Adv. Drug Deliv. Rev. 24 (1997) 337–344.

[14] Y. Sadzuka, S. Nakai, A. Miyagishima, Y. Nozawa, S. Hirota, The effect of dose on the distribution of adriamycin encapsulated in polyethyleneglycol-coated liposomes, J. Drug Target. 3 (1995) 31–37.

[15] A.S. Derycke, P.A. de Witte, Liposomes for photodynamic therapy, Adv. Drug Deliv. Rev. 56 (2004) 17–30.

[16] B. Ludovic, T. Sonia, F. Monica, F. Yann, S. Gerard, P. Thierry, In vivo photosensitizing efficiency of a diphenylchlorin sensitizer: interest of a DMPC liposome formulation, Pharm. Res. 47 (2003) 253–261.

[17] F. Jiang, L. Lilge, B. Logie, Y. Li, M. Chopp, Photodynamic therapy of 9L gliosarcoma with liposome-delivered photofrin, Photochem. Photobiol. 65 (1997) 701–706.

[18] F. Jiang, L. Lilge, J. Grenier, Y. Li, M.D. Wilson, M. Chopp, Photodynamic therapy of U87 human glioma in nude rat using liposome-delivered photofrin, Laser Surg. Med. 22 (1998) 74–80.

[19] A. Igarashi, H. Konno, T. Tanaka, S. Nakamura, Y. Sadzuka, T. Hirano, et al., Liposomal photofrin enhances therapeutic efficacy of photodynamic therapy against the human gastric cancer, Toxicol. Lett. 145 (2003) 133–141.

[20] E. Gross, B. Ehrenberg, F.M. Johnson, Singlet oxygen generation by porphyrins and the kinetics of 9,10-dimethylanthracene photosensitization in liposomes, Photochem. Photobiol. 57 (1993) 808–813.

[21] A.D. Bangham, M.M. Standish, J.C. Watlcins, Diffusion of univalent ion across the lamellae of swollen phospholipids, J. Mol. Biol. 13 (1965) 238–252.

[22] G.C. Lin, M.L. Tsoukas, M.S. Lee, S. Gonzalez, G. Vibhagool, R.R. Anderson, et al., Skin necrosis due to photodynamic action of benzoporphyrin depends on circulating rather than tissue drug levels: implications for control of photodynamic therapy, Photochem. Photobiol. 68 (1998) 575–583.

[23] Wong Zhi-Jin, He Yu-Ying, Huang Chao-Guo, Huang Jin-Sheng, Huang Ying-Sheng, Huang Ying-Cai, et al., Pharmacokinetics, tissue distribution and photodynamic therapy efficacy of liposomal-delivered Hypocrellin A, a potential photosensitizer for tumor therapy, Photochem. Photobiol. 70 (1999) 773–780.

[24] M.H. Reinke, C. Canakis, D. Husain, N. Michaud, T.J. Flotte, E.S. Gragoudas, et al., Verteporfirin photodynsmic therapy reteament of nomal retina and choroids in the cynomolgus monkey, Ophthalmology 106 (1999) 1915–1923.

[25] A.V. Reshetnikov, I.V. Zhigaltsev, S.N. Kolomeichuk, A.P. Kaplun, V.I. Shvets, O.S. Zhukava, et al., Preparation and certain properties of the liposomal substance 2,4-di(1-methyl-3-hydroxybutyl)- deuterporphyrin-IX, Bioorg. Khim. 25 (10) (1999) 782–790.

[26] L. Lile, B.C. Wilson, Photodynamic therapy of intracranial tissues: a preclinical comparative study of four different photosensitizers, J. Clin. Laser Med. Surg. 16 (1998) 81–91.

[27] A. Gijsens, A. Derycke, L. Missiaen, D.D. Vos, J. Huwyler, A. Eberle, et al., Targeting of the photocytotoxic compound AlPcS4 to hela cells by transferring conjugated PEG-liposomes, Int. J. Cancer 101 (2002) 78–85.

[28] H. Konno, A. Igarashi, T. Tanaka, S. Nakamura, Y. Sadzuka, T. Hirano, et al., Liposomal photofrin enhances therapeutic efficacy of photodynamic therapy against the human gastric cancer, 93th AACR, Abstracts, 2002, p. 651.

DDSにおける基盤技術開発

リポソーム応用の新展開

浅井知浩*　奥　直人**

要　旨

本稿では，がん化学療法および遺伝子治療法におけるリポソーム研究の現状を述べ，そして我々の最近の研究成果についても紹介したい．ここでは「標的化リポソームによる腫瘍新生血管傷害療法」および「ポリカチオンリポソームを用いたsiRNAデリバリー」に関する研究を中心に述べる．リポソーム研究は，近年脚光を浴びているナノメディシン研究領域においても注目を集めており，がんの革新的治療法につながることが期待されている．

がん領域におけるリポソームDDS

リポソームは生体適合性や利便性が高く，薬物や核酸あるいはタンパク質などのキャリヤーとして多くの疾患領域において応用が試みられている．中でもがん領域における研究が最も盛んになされており，抗がん剤を含有したリポソーム製剤は欧米において複数品目が承認されている．具体的には，Doxil®（適応：カポジ肉腫，転移性乳がん，難治性卵巣がん，欧名：Caelyx），DaunoXome®（適応：カポジ肉腫），およびMyocet®（適応：転移性乳がん）がこれに該当する．しかし日本においては，がんを対象としたリポソーム製剤に臨床試験段階のものはあっても，現在のところ上市に至ったものはない．日本で承認されたリポソーム製剤は，加齢性黄斑変性症を適応とする光線力学療法（photodynamic therapy：PDT）用のVisudyne®だけである．現在，深在性真菌症治療薬AmBisome®が申請中となってはいるが，日本では全般的にリポソーム製剤の開発が遅れており，それはがん領域においても残念ながら同様である．

ところで，リポソームは抗がん剤以外の医薬品，試薬，化粧品などに関してもすでに実用化されており，広範な目的で利用されている．近年ではリポソームを利用した人工血液細胞（人工血小板および人工赤血球）の創製に関しても，実用化の可能性が高まってきている．さらにリポソームは，新しいタイプの核酸医薬として非常に大きな期待を集めているshort interfering RNA（siRNA）のベクターとしても，研究開発が鋭意進行している．siRNAを利用した治療は，がん領域においても革新的な治療法の開発につながる可能性がある．リポソームは実用化されてから久しいが，このように依然としてナノメディシン

* 静岡県立大学薬学部 医薬生命化学教室 講師
** 同 教授

キーワード：腫瘍新生血管標的化リポソーム，腫瘍新生血管傷害療法，ポリカチオンリポソーム，siRNAデリバリー